MODELING THE EFFECTS OF DRUGS OF ABUSE ON HIV INFECTIONS WITH TWO VIRAL SPECIES

A THESIS IN
Mathematics
and
Statistics

Presented to the Faculty of the University
of Missouri-Kansas City in partial fulfillment of
the requirements for the degree

MASTER OF SCIENCE

by
PETER MAURICE UHL

B.S., University of Missouri-Kansas City, 2015

Kansas City, Missouri
2017

MODELING THE EFFECTS OF DRUGS OF ABUSE ON HIV INFECTIONS WITH TWO VIRAL SPECIES

Peter Maurice Uhl, Candidate for the Master of Science Degree

University of Missouri-Kansas City, 2017

ABSTRACT

Injection drug use is one of the greatest risk factors associated with contracting human immunodeficiency virus (HIV), and drug abusers infected with HIV suffer from a higher viral load and rapid pathogenesis. Replication of HIV may result in a large number of mutant viruses that can escape recognition of the hosts immune response. Experimental results have shown that the presence of morphine can decrease the viral mutation rate and cellular immune responses. This thesis presents a mathematical model to determine if the decrease in mutation and cellular immune response in the presence of morphine can account for the increased viral load. Two viral species are considered: a wild-type and a mutant. The morphine-altered mutation rate and cellular immune response is shown to allow the wild-type virus to out compete the mutant, resulting in a higher set point viral load. Calculation of the basic reproduction number for each species shows that the dominant species is determined by a threshold morphine concentration, with the mutant dominating below the threshold and the wild-type dominating above. Stability analysis is performed on the infection free and mutant only equilibria of the system and numerical simulations reflect the

increased viral load associated with morphine use.

The faculty listed below, appointed by the Dean of College of Arts and Science, have examined a thesis titled "Modeling the Effects of Drugs of Abuse on HIV Infections with Two Viral Species", presented by Peter Maurice Uhl, candidate for the Master of Science degree, and certify that in their opinion it is worthy of acceptance.

Supervisory Committee

Naveen K. Vaidya, Ph.D., Committiee Chair
Department of Mathematics and Statistics

Noah Rhee, Ph.D.
Department of Mathematics and Statistics

Majid Bani-Yaghoub, Ph.D.
Department of Mathematics and Statistics

CONTENTS

ILLUSTRATIONS

TABLES

ACKNOWLEDGMENTS

I would like to thank my committee members Dr. Rhee and Dr. Bani for their input into this thesis, Larry Eifler for creating the LATEX template used, and Anil Kumar for the experiment this work was based in part on. I especially want to thank my supervisor Dr. Vaidya for all of his guidance and support during my time at UMKC.

CHAPTER 1

INTRODUCTION

Human immunodeficiency virus (HIV) is a significant health concern in the United States and around the world, with some $56,000$ new infections per year in the United States [1]. HIV is a blood borne pathogen and one of the most common forms of transmission is by the sharing of needles used for injecting cocaine or heroin between infected and non- infected persons. Drugs of abuse have been shown to have adverse effects on the progression of HIV infections, including a higher set point viral load and decreased amounts of CD4+ T cells [2]. Studies involving rhesus macaques and simian immunodeficiency virus (SIV) have shown that morphine causes a faster progression to AIDS and pathogenesis in morphine affected animals, and studies of HIV have also demonstrated a quicker progression to AIDS associated with opiate use [3]. It is therefore important to investigate the mechanisms by which morphine affects the progression of HIV infections.

Cytotoxic T-lymphocytes (CTLs) are an important component of the human immune system for combating viral infections, including HIV, by limiting viral reproduction and the infection of hosts target cells, therefore the production of CTLs plays a significant role in the progression of an infection [4]. However, HIV possesses a high genetic variability which results in the production of escape mutants that can avoid detection by CTLs [5]. Continuous infection of target cells also results in a large amount of newly infected cells and free virus particles [6]. As a result, the production

of mutant viruses is a significant barrier to the treatment of HIV by antiviral drugs or to the development of an effective vaccine [5].

Mathematical models have been very useful in understanding the dynamics of infectious diseases [6, 7]. A problem on which there has been little study is to determine the effects of morphine on the viral dynamics of HIV when multiple viral species are present, and the objective of this thesis is to present such a model. This thesis is organized as follow: Chapter 2 will introduce the relevant biological concepts and mathematical modeling of HIV dynamics, Chapter 3 will develop a novel mathematical model that incorporates immune escape and morphine effects into an HIV dynamics model, Chapter 4 will introduce the basic reproduction number and discuss the steady state solutions of the model, Chapter 5 will present some numerical simulations of the model and discuss short- and long-term viral dynamics, and Chapter 6 will be a discussion of the results and future works.

CHAPTER 2

BACKGROUND AND LITERAURE REVIEW

HIV Infections and Drugs of Abuse

The target cells of HIV are CD4+ T cells, which are a part of the immune system that signal other immune cells to attack foreign antigens when they are present [8, 9]. HIV virions attack CD4+ cells by attaching to receptors on the CD4+ cell surface and entering the interior of the cell, where the virions can begin reproducing [10]. Once the virus has entered a target cell, the target cell becomes infected and begins releasing new virions. The early stages of infection are characterized by a rapid production of a large number of virions and infected cells [11], making the early weeks of infection crucial in determining the long-term viral dynamics.

In the acute stage of the infection the hosts immune system responds by creating a large amount of virus specific CTLs. The CTLs perform actions to inhibit viral growth, for example producing cytokines that limit viral reproduction, reducing the amount of receptors available on target cells, and by destroying infected cells directly, but it is not clear which actions are the most important for combating acute HIV infections [12]. The high number of CTLs puts pressure on the virus to quickly mutate to a form that can evade the CTLs, this combined with the quick replication speed of HIV results in a large number of mutant viruses being produced [13, 14]. After the infection has progressed and the immune response by CTLs has been reduced it is possible for mutant viruses to revert back to the original wild-type strain.

Experimental studies have shown that opiates can increase viral replication by increasing CCR5 expression in target cells [15] and studies on rhesus macaques have shown similar levels of viral growth in the early stages of infection between morphine dependent and control animals, but higher set point viral loads associated with morphine use [2]. Morphine has also been shown to affect the amount of escape mutants that evolve, but the exact effect remains unclear [16]. Thus, it is desirable to develop a mathematical model that will include components for the hosts cellular immune response (CTLs), escape mutations, and morphine use.

Viral Dynamics Modeling

Deterministic differential equations are used extensively to model infectious disease, and a similar approach will be used here. The simplest HIV model is given by

$$\begin{aligned} T' &= \lambda - \beta VT - \delta_T T \\ V' &= pI - \delta_V V \\ I' &= \beta VT - \delta_I I \end{aligned}$$

Where T, I, and V are the populations of target cells, infected cells, and free virions, respectively, and a prime denotes the derivative with respect to time, in days. Target cells are produced at constant rate λ and die naturally at rate δ_T per cell. Infected cells are produced via the mass action term βTV proportional to the number of target cells and free virions. Free virions are produced at rate pI proportional to the number of infected cells. Target cells, infected cells, and free virions die at rates $\delta_T T$, $\delta_I I$, and $\delta_V V$, respectively [6, 20].

Vaidya et al. [21] developed a model that incorporates two separate target cell subpopulations based on the experimental observation that morphine can increase the co-receptor expression of certain target cells and make them more susceptible to infection and that individual cells can transition between these subpopulations [21]. The differential equations for this model are

$$\begin{aligned} T_l' &= \lambda + qT_h - rT_l - \beta_l V T_l - \delta_T T_l \\ T_h' &= rT_l - qT_h - \beta_h V T_h - \delta_T T_h \\ V' &= pI - \delta_V V \\ I' &= \beta_l V T_l + \beta_h V T_h - \delta_I I \end{aligned}$$

The two subpopulations of target cells are denoted T_l and T_h and have corresponding infection terms $\beta_l V T_l$ and $\beta_h V T_h$. The subpopulations are distinguished by their different suseptibilities to infection induced by morphine use, with T_l having lower susceptibility and T_h having higher susceptibility. Target cells transistion between subpopulations at rates qT_h from T_h to T_l and rT_l from T_l to T_h.

Konrad et al. [19] developed a model to study the effectiveness of a CTL based vaccine that included a wild-type virus V_w, a mutant virus V_m, and a cellular immune response in the form of CTLs. In their model, the total viral load is divided into subpopulations of wild-type and mutant virus with corresponding subpopulations of infected cells. This model accounts for immune response by including a population of CTLs, C, the production of which is stimulated by the presence of infected cells and which kill infected cells at rates proportional to the populations of CLTs and infected cells.

CHAPTER 3

MATHEMATICAL MODELS

This chapter will develop a novel mathematical model that incorporates the effects of morphine on the viral mutation rate and the CTL proliferation rate into existing HIV models, then give a description of the parameters of the model.

Model Formulation

Modifying the model from Vaidya et al. [21] to include populations of wild-type viruses, mutant viruses, and CTLs results in the system

$$\begin{aligned}
T_l' &= \lambda + qT_h - rT_l - \beta_l V_w T_l - \hat{\beta}_l V_m T_l - \delta_T T_l \\
T_h' &= rT_l - qT_h - \beta_h V_w T_h - \hat{\beta}_h V_m T_h - \delta_T T_h \\
V_w' &= pI_w - \delta_V V_w \\
V_m' &= pI_m - \delta_V V_m \\
I_w' &= (1-\epsilon)(\beta_l V_w T_l + \beta_h V_w T_h) - bI_w C - \delta_I I_w \\
I_m' &= \epsilon(\beta_l V_w T_l + \beta_h V_w T_h) + \hat{\beta}_l V_m T_l + \hat{\beta}_h V_m T_h \\
&\quad -\hat{b} I_m C - \delta_I I_m \\
C' &= \omega + \alpha(I_w + I_m)C - \delta_C C
\end{aligned}$$

Target cells interact with free virions to produce actively infected cells via infection; target cells are divided into subpopulations T_l, which are less susceptible to infection due to lower co-receptor expression, and T_h which are more susceptible to infection. Target cells transition from T_h to T_l at rate qT_h and from T_l to T_h at rate

rT_l [21]. It is assumed that newly created target cells are all in the T_l subpopulation and are produced at constant rate λ [6, 21]. Wild-type virions infect T_l target cells at rate $\beta_l V_w T_l$, where β_l is the per capita infection rate of T_l by the wild-type virus. Mutant virions infect T_l target cells at rate $(1-F)\beta_l V_m T_l$, where F is the fitness cost of the mutant virus- a reduction in the mutant's infection rate relative to the wild-type's caused by mutation[26]. Similarly, T_h cells are infected by wild-type and mutant viruses at rates $\beta_h V_w T_h$ and $(1-F)\beta_h V_m T_h$, respectively, where β_h is the per capita infection rate of T_h by the wild-type virus [19]. Target cells die naturally at rates $\delta_T T_l$ and $\delta_T T_h$ corresponding to T_l and T_h [27, 19].

When target cells are infected by either the wild-type virus V_w or the mutant virus V_m they become actively infected cells I_w and I_m, at which point there is no distinction based on levels of co-receptor expression. In the model developed by Konrad et al [19], a portion of target cells infected by the wild-type virus mutate and become mutant infected cells rather than wild-type infected cells based on the mutation parameter ϵ. The parameters μ and η are introduced to model the lowered mutation rate caused by morphine [16] so that the per capita mutation rate becomes $\frac{\epsilon}{\mu+\eta M}$, where M is the concentration of morphine which, for simplicity, is assumed to be constant. Therefore, wild-type infected cells are produced at rate $(1-\frac{\epsilon}{\mu+\eta M})(\beta_l V_w T_l + \beta_h V_w T_h)$, while the remainder $\frac{\epsilon}{\mu+\eta M}(\beta_l V_w T_l + \beta_h V_w T_h)$ are converted into mutant infected cells. Mutant infected cells are additionally produced by way of infection of target cells by mutant virions at the total rate of $(1-F)(\beta_l V_m T_l + \beta_h V_m T_h)$. Infected cells die at rates $\delta_I I_w$ and $\delta_I I_m$. Wild-type and mutant infected cells produce free virions, V_w and V_m, which are cleared at rates

$\delta_V V_w$ and $\delta_V V_m$, respectively [27, 19].

Due to different epitote mutations, CTLs are assumed to be produced at constant rate ω and also to reproduce in the presense of infected cells [19]. Konrad et al. denote α as the rate of CTL production in response to the total amount of infected cells $I_w + I_m$. The parameters γ and ξ are introduced to lower the CTL production rate [2], changing the CTL produciton rate to $\frac{\alpha}{\gamma+\xi M}(I_w + I_m)C$. CTLs kill wild-type infected cells at rate bI_wC, where b is the per capita wild-type clearance rate. Due to responses by epitope-specific CTLs there is some recognition of the mutant by the CTL response [19, 28], so the clearance rate of the mutant virus is assumed to be $\frac{b}{B}I_mC$, where B represents the escape ratio- a reduction in the ability of CTLs to kill mutant infected cells. CTLs die at rate $\delta_C C$. Since the viral speices are distinguished only by the fitness cost of the mutant, F, and the escape ratio, B, it is only neccessary to consider two populations of virus.

The model can be written as the following system of differential equations:

$$\begin{aligned}
T_l' &= \lambda + qT_h - rT_l - \beta_l V_w T_l - (1-F)\beta_l V_m T_l - \delta_T T_l \\
T_h' &= rT_l - qT_h - \beta_h V_w T_h - (1-F)\beta_h V_m T_h - \delta_T T_h \\
V_w' &= pI_w - \delta_V V_w \\
V_m' &= pI_m - \delta_V V_m \\
I_w' &= (1 - \tfrac{\epsilon}{\mu+\eta M})(\beta_l V_w T_l + \beta_h V_w T_h) - bI_wC - \delta_I I_w \\
I_m' &= \tfrac{\epsilon}{\mu+\eta M}(\beta_l V_w T_l + \beta_h V_w T_h) + (1-F)(\beta_l V_m T_l + \beta_h V_m T_h) \\
&\quad -\tfrac{b}{B}I_mC - \delta_I I_m \\
C' &= \omega + \tfrac{\alpha}{\gamma+\xi M}(I_w + I_m)C - \delta_C C
\end{aligned}$$

For simplicity, the notation $\hat{\beta}_l = (1-F)\beta_l$, $\hat{\beta}_h = (1-F)\beta_h$, $\hat{\epsilon} = \frac{\epsilon}{\mu+\eta M}$, and

$\hat{\alpha} = \frac{\alpha}{\gamma+\xi M}$ will sometimes be used.

Parameter Descriptions

Vaidya et al. [21] provides that there are approximately 10^6 target cells initially per ml of blood, with about $40980/ml$ belonging in the T_l population and the remaining $10^6 - 40980/ml$ in the T_h population. They also estimate an initial viral load of 200 viral RNA copies per ml, which is here assumed to all belong to the wild-type population. Since there is initally no infection, I_w, I_m, and C are all initially zero. Additionally, they provide estimates for λ of $3690/ml$ per day, $r = 0.16$ cells per day, and $q = 0.24$ cells per day when morphine is not present and $r = 0.55$ cells per day and $q = 1.02 \times 10^{-6}$ cells per day when morphine is present. The wild-type infection rate of T_l, β_l, is estimated to be on the order of $10^{-9}ml$ per day and the wild-type infection rate of T_h, β_h approximately two orders of magnitude higher. Finally, they estimate the death rate of infected cells δ_I as between 0.31 and 0.78 cells per day and the common production rate of the viruses as $p = 2500$ virions per day. The infection rates of T_l and T_h by the mutant virus is calculated as a percentage of the corresponding infection rate of the wild-type virus, giving $(1-F)\beta_l$ and $(1-F)\beta_h$ where the fitness cost F is a number between zero and one [6].

Ramratnam et al. [29] estimate the average virion clearance rate as 23 cells per day, giving $\delta_V = 23$ [29] and Stafford et al. [30] provide the average target cell life span as 100 days, giving $\delta_T = 0.01$ [30]. This model assumes that only forward mutation takes place, i.e., that mutant infected cells will not mutate back into the wild-type infected population. The forward mutation rate ϵ has been observed experimentally to be 3×10^{-5} in [31], the parameters μ and η that account for the effect of morphine

on ϵ will be varied. De Boer and Perelson [33] estimated the CTL proliferation rate as $\alpha = 6.7^{-5}ml$ per day, and as before the parameters γ and ξ accounting for the effect of morphine will vary. Konrad et al. [19] take δ_C on the order of 10^{-1} cells per day and the rate of killing of wild- type infected cells on the order of 10^{-2}, the escape ratio B will be varied.

The constant rate of CTL production ω is assumed to be 50 cells per day and to decay exponentially when morphine is present, therefore the parameter ψ is introduced as the decay rate giving $\hat{\omega} = \omega e^{-\psi M}$ when morphine is present. Olkkola et al. [23] measured the kinetics and dynamics of morphine in children and observed initial concentrations of morphine between $28 - 325\mu l$ per kilogram of body weight, therefore $300\mu l/kg$ is taken as a reasonable morphine concentration.

The parameter descriptions are summarized in Table 1:

Table 1. Parameter Values

Parameter	Value	Description	Reference
λ	3690 $ml^{-1}day^{-1}$	Production rate of T_l cells	Vaiyda et al.
r	0.16 day^{-1}	Conversion of T_l to T_h	Vaiyda et al.
q	0.24 day^{-1}	Conversion of T_h to T_l l	Vaiyda et al.
β_l	$10^{-9}cells^{-1}ml\ day^{-1}$	Wild- type infection rate of T_l cells	Vaiyda et al.
β_h	$10^{-7}cells^{-1}ml\ day^{-1}$	Wild -type infection rate of T_h cells	Vaiyda et al.
F	$0-1$	Fitness cost of mutation	Varied
p	2500 day^{-1}	Production rate of virus	Vaiyda et al.
b	0.005 $cells^{-1}ml\ day^{-1}$	CTL killing rate of wild- type	Konrad et al.
B	$1-100$	Escape ratio	Varied
α	$6.7\times10^{-6}\ cells^{-1}\ ml\ day^{-1}$	CTL proliferation rate	De Boer et al.
γ	$0.4-1$	Morphine parameter affecting α	Varied
ξ	$0.4-1$	Morphine parameter affecting α	Varied
ω	50	CTL production rate	Varied
ψ	0.05	CTL prduction decay rate	Varied
ϵ	3×10^{-5}	Mutation rate	Mansky et al.
μ	$0.1667-1$	Morphine parameter affecting ϵ	Varied
η	$0.1667-1$	Morphine parameter affecting ϵ	Varied
δ_T	0.01 day^{-1}	Target cell death rate	Stafford et al.
δ_V	23 day^{-1}	Virus clearance rate	Ramratnam et al.
δ_I	0.3 day^{-1}	Infected cell death rate	Vaidya et al.
δ_C	0.63 day^{-1}	CTL death rate	Konrad et al.
M	$0-400\ ml/kg$	Concentration of morphine	Olkkola et al.

CHAPTER 4

MODEL ANALYSIS

This chapter will discuss the stability of two equilibira of the model: the infection free equilibrium and the mutant only equilibrium, determine their local stability, and demonstrate that there is no biologically relevant wild-type only equilibrium. The local stability of the infection free equilibrium will be determined by calculating the basic reproduction number of the virus, the local stability of the mutant only equilibrium will be determined by calculating the eigenvalues of the Jacobian matrix of the model evaluated at the mutant only equilibrium.

Basic Reproduction Number

The basic reporduction number is an important quantity in the study of viral dynamics and is defined as the average number of secondary infections resulting from a single initial infection [22]. Determining the long-term behavior of infections involves studying the equilibria of differential equations, and models of viral dynamics generally have at least two equilibria: an infection free equilbrium and an infected equilbrium. The stability of the infection free equilibrium (IFE) can be described by the basic reporduction number, denoted R_0, with the IFE being locally asymptotically stable if $R_0 < 1$ and unstable if $R_0 > 1$ [22]. That is, if an initial infection on average results in less than one secondary infections the infection will die out. Since this model contains two viral species the basic reproduction number is a combination of the two quantities R_0^w and R_0^m, the reproduction numbers corresponding to the

wild-type and mutant viruses, respectively.

The IFE of is the constant solution of the system in which there is no virus present, so it is of the form $(T_l^*, T_h^*, 0, 0, 0, 0, C^*)$ and is obtainted by solving the algebraic system

$$\begin{aligned} 0 &= \lambda + qT_h^* - rT_l^* - \delta_T T_l^* \\ 0 &= rT_l - qT_h^* - \delta_T T_h^* \\ 0 &= \omega - \delta_C C^* \end{aligned}$$

which yields

$$\begin{aligned} T_l^* &= \tfrac{\lambda(q+\delta_T)}{\delta_T(q+r+\delta_T)} \\ T_h^* &= \tfrac{\lambda r}{\delta_T(q+r+\delta_T)} \\ C^* &= \tfrac{\omega}{\delta_C}. \end{aligned}$$

The method of calculating the basic reproduction number used here is by constructing the next-generation matrix of the model and caluculating its spectral radius. The next-generation matrix is obtained from the infected subsystem of the model; the equations of the system that contain viruses and infected cells [34]. For this model, the infected subsystem is given by

$$\begin{aligned} V_w' &= pI_w - \delta_V V_w \\ V_m' &= pI_m - \delta_V V_m \\ I_w' &= (1-\hat{\epsilon})(\beta_l V_w T_l + \beta_h V_w T_h) - bI_w C - \delta_I I_w \\ I_m' &= \hat{\epsilon}(\beta_l V_w T_l + \beta_h V_w T_h) + (\hat{\beta}_l V_m T_l + \hat{\beta}_h V_m T_h) - \tfrac{b}{B} I_m C - \delta_I I_m \end{aligned}$$

The next step is to calculate the Jacobian matrix of the infected subsystem

and decompose it into $\mathcal{F}-\mathcal{V}$, where $\mathcal{F}$ is the infection part of the system which describes newly infected components and $\mathcal{V}$ is the transition part, which describes transitions of infected components between populations of the model. For this model, $\mathcal{F}$ and $\mathcal{V}$ are given by

$$\mathcal{F} = \begin{bmatrix} 0 & 0 & 0 & 0 \\ 0 & 0 & 0 & 0 \\ (1-\hat{\epsilon})(\beta_l T_l^* + \beta_h T_h^*) & 0 & 0 & 0 \\ \hat{\epsilon}(\beta_l T_l^* + \beta_h T_h^*) & \hat{\beta}_l T_l^* + \hat{\beta}_h T_h^* & 0 & 0 \end{bmatrix}$$

and

$$\mathcal{V} = \begin{bmatrix} \delta_V & 0 & -p & 0 \\ 0 & \delta_V & 0 & -p \\ 0 & 0 & \delta_I + bC^* & 0 \\ 0 & 0 & 0 & \delta_I + \frac{b}{B}C^* \end{bmatrix}.$$

The next generation matrix is then given by $\mathcal{F}\mathcal{V}^{-1}$ and its specral radius is the basic reproduction number of the system. The spectrum of $\mathcal{F}\mathcal{V}^{-1}$ was obtained using the computer algebra system in Maple and is shown below:

$$\sigma(\mathcal{F}\mathcal{V}^{-1}) \quad = \quad \begin{bmatrix} 0 \\ 0 \\ -\frac{p(T_h^*\beta_h\hat{e}+T_l^*\beta_l\hat{e}-T_h^*\beta_h-T_l^*\beta_l}{(\delta_I+bC^*)\delta_V} \\ -\frac{pB(FT_h^*\beta_h+FT_l^*\beta_l-T_h^*\beta_h-T_l^*\beta_l}{B\delta_I+bC^*)\delta_V} \end{bmatrix}$$

where the thrid entry corresponds to R_0^w and the fourth to R_0^m. The basic reproduction number is then $R_0 = \max(R_0^w, R_0^m)$ and the IFE is locally asymptotically stable provided $R_0^w < 1$ and $R_0^m < 1$ and unstable otherwise. Sensitivity analysis can be done on the parameters in order to identify those that have the greatest effect on the basic reporduction number. [32]. For a parameter x, the forward sensitivity index is given by [36, 35]

$$S_x \quad = \quad \frac{x}{R_0}\frac{\partial R_0}{\partial x} \quad .$$

Using the parameter values in Table 1, the sensitivity indecies for R_0^w and R_0^m are given in Table 2. Based on Table 2, increasing λ and p increases both R_0^w and R_0^m significantly while increasing δ_V, δ_I, and δ_T decreases both R_0^w and R_0^m significantly.

Dominant Viral Species

In order to observe the effect of morphine on R_0, and therefore on the viral load, R_0^w and R_0^m are calculated for various concentrations of morphine, noting that if $R_0^w > R_0^m$ the wild-type virus will be the dominate viral species while if $R_0^w < R_0^m$ the mutant will dominate. Using the Parameter values in Table 1 and letting M vary

Table 2. Sensitivity Indices

	R_0^w	R_0^m
x	S_x	S_x
λ	1	1
q	-0.5705966223	-0.5705966226
r	0.01538461539	0.5943714821
β_l	0.01538461539	0.01538461538
β_h	0.9846153847	0.009846153846
p	1	1
b	$-4.046294658 \times 10^{-7}$	$-4.046246133 \times 10^{-8}$
B	NA	$3.939487339 \times 10^{-8}$
δ_T	-1.023774858	-1.023774859
δ_V	-1	-1
δ_I	-0.9999995953	-0.9999999598
δ_C	$4.051855513 \times 10^{-7}$	$1.057200164 \times 10^{-8}$
ϵ	$-9.94476127 \times 10-7$	NA
μ	$5.494167551 \times 10^{-9}$	NA
F	NA	-0.25

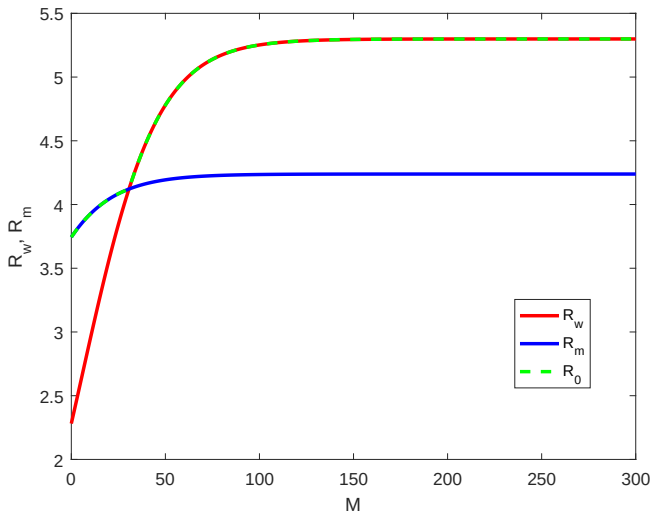

Figure 1. Computed values of R_w and R_m for increasing M. A population switch occurs at approximately $M = 31$.

from 0 to 300 gives the results shown Figure 1.

Setting $M = 0$ results in $R_0^m = 3.7439$ and $R_0^w = 2.2812$, indicating that the mutant virus is dominate when there is no morphine and that the IFE is unstable. A population switch occurs at approximately $M = 31$ and the mutant becomes dominant for any higher morphine concentrations. In the next chapter, simulations of the steady state viral load will show that the dominance of the mutant virus contributes to the higher viral load when mophine is present.

Mutant Only Equilbirum

The mutant only equilibrium (MOE) is the equilibrium in which there is no wild-type virus present and is of the form $(T_l^*, T_h^*, 0, V_m^*, 0, I_m^*, C^*)$. Note that because

of the mutation term in the equation for I_m some mutant virus is being produced whenever the wild-type virus is present and for this reason there is no positive wild-type only equilibrium. The mutant only equilbrium is calculated by solving the system

$$\begin{aligned}
0 &= \lambda + qT_h^* - rT_l^* - \hat{\beta}_l V_m^* T_l^* - \delta_T T_l^* \\
0 &= rT_l^* - qT_h^* - \hat{\beta}_h V_m^* T_h^* - \delta_T T_h^* \\
0 &= pI_m^* - \delta_V V_m^* \\
0 &= \hat{\beta}_l V_m^* T_l^* + \hat{\beta}_h V_m^* T_h^* - \tfrac{b}{B} I_m^* C^* - \delta_I I_m^* \\
0 &= \omega + \hat{\alpha} I_m^* C^* - \delta_C C^*
\end{aligned}$$

which yields

$$\begin{aligned}
T_h^* &= \frac{\lambda}{(q+\hat{\beta}_h+\delta_T)\cdot[1+\frac{\hat{\beta}_l V_m^*}{r}+\frac{\delta_T}{r}-q]} \\
T_l^* &= T_h^* \cdot \frac{q+\hat{\beta}_h V_m^*+\delta_T}{r} \\
I_m^* &= \frac{\delta_V V_m^*}{p} \\
C^* &= \frac{\omega}{\delta_C - \hat{\alpha} I_m^*}
\end{aligned}$$

where V_m^* is the solution of

$$\begin{aligned}
0 = {} & \hat{\beta}_l V_m^* [T_h^* \tfrac{q+\hat{\beta}_h V_m^*+\delta_T}{r}] + \hat{\beta}_h V_m^* T_h^* \\
& - \tfrac{b}{B}(\tfrac{\delta_V V_m^*}{p})(\tfrac{\omega}{\delta_C - \hat{\alpha}(\frac{\delta_V V_m}{p})}) - \tfrac{\delta_I \delta_V V_m}{p}.
\end{aligned}$$

Substituting T_h^* and solving numerically gives a value for V_m^*. Several values of V_m^* are plotted in Figure 2 for different values of M. Notably, increased values of M cause an increase in V_m^* and a decrease in C^*. For all values in Table 2, $F = 0.2$

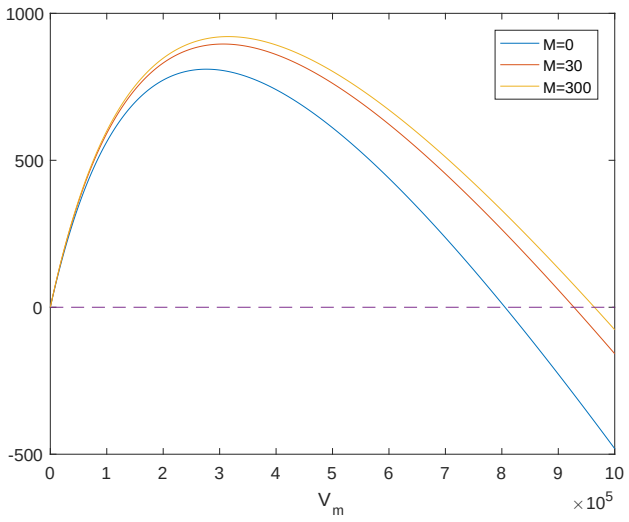

Figure 2. Solutions of V_m^* equation. The zero-intercept of each curve is the MOE value of V_m for the particular value of M.

Table 3. Mutant Only Equilibrium

	$M = 0$	$M = 30$	$M = 300$
V_m	8.058×10^5	9.277×10^5	9.64×10^5
T_h	3.8685×10^4	3.4817×10^4	3.3809×10^4
T_l	7.6032×10^4	7.0551×10^4	6.9123×10^4
I_m	7.413×10^3	8.5348×10^3	8.868×10^3
C	86.1578	17.7607	2.4286×10^{-5}

and $B = 10$.

To determine the stability of the MOE, the Jacobian matrix is calculated and evaluated at the MOE. The Jacobian matrix is

$$J = \begin{bmatrix} J_{11} & J_{12} & J_{13} & J_{14} & 0 & 0 & 0 \\ J_{21} & J_{22} & J_{23} & J_{24} & 0 & 0 & 0 \\ 0 & 0 & J_{33} & 0 & J_{35} & 0 & 0 \\ 0 & 0 & 0 & J_{44} & 0 & J_{46} & 0 \\ J_{51} & J_{52} & J_{53} & 0 & J_{55} & 0 & J_{57} \\ J_{61} & J_{62} & J_{63} & J_{64} & 0 & J_{66} & J_{67} \\ 0 & 0 & 0 & 0 & J_{75} & J_{76} & J_{77} \end{bmatrix}$$

where

$$\begin{aligned} J_{11} &= -r - \beta_l V_w - \hat{\beta}_l V_m - \delta_T \\ J_{12} &= q \\ J_{13} &= -\beta_l T_l \\ J_{14} &= -\hat{\beta}_l T_l \\ J_{21} &= r \\ J_{22} &= -q - \beta_h V_w - \hat{\beta}_h V_m - \delta_T \\ J_{23} &= -\beta_h T_h - \hat{\beta}_h T_h \\ J_{24} &= -\hat{\beta}_h T_h \\ J_{33} &= -\delta_V \\ J_{35} &= p \\ J_{44} &= -\delta_V \\ J_{46} &= p \\ J_{51} &= (1 - \hat{\epsilon})\beta_l V_w \\ J_{52} &= (1 - \hat{\epsilon})\beta_h V_w \end{aligned}$$

$$
\begin{aligned}
J_{53} &= (1-\hat{\epsilon})(\beta_l T_l + \beta_h T_h) \\
J_{55} &= -bC - \delta_I \\
J_{57} &= -bI_w \\
J_{61} &= \hat{\epsilon}\beta_l V_w + \hat{\beta}_l V_m \\
J_{62} &= \hat{\epsilon}\beta_h V_w + \hat{\beta}_h V_m \\
J_{63} &= \hat{\epsilon}(\beta_l T_l + \beta_h T_h) \\
J_{64} &= \hat{\beta}_l T_l + \hat{\beta}_h T_h \\
J_{66} &= -\tfrac{b}{B} C - \delta_I \\
J_{67} &= -\tfrac{b}{B} I_m \\
J_{75} &= \hat{\alpha} C \\
J_{76} &= \hat{\alpha} C \\
J_{77} &= \hat{\alpha}(I_w + I_m) - C.
\end{aligned}
$$

The MOE is locally asymptotically stable if the real parts of each eigenvalue of J is negative and unstable otherwise [24, 27]. For $M = 0$,

$$
\begin{aligned}
\sigma(J((T_l^*, T_h^*, 0, V_m^*, 0, I_m^*, C^*))) &= \{-23.3439, -0.0349 \pm 0.0894i, -0.5773, \\
&\quad -0.4175, -23.4343, -0.2967\}
\end{aligned}
$$

and for $M = 30$

$$
\begin{aligned}
\sigma(J((T_l^*, T_h^*, 0, V_m^*, 0, I_m^*, C^*))) &= \{-23.3099, -0.0351 \pm 0.0894i, -0.6281, \\
&\quad -0.4238, -23.3832, -0.0026\}
\end{aligned}
$$

so the MOE is locally asymptotically stable for these values of M, but $M = 300$ results in

$$\begin{aligned}\sigma(J((T_l^*, T_h^*, 0, V_m^*, 0, I_m^*, C^*))) &= \{-23.3010, -0.0357 \pm 0.0895i, -0.4255, \\ &\quad -0.6298, -23.3738, 0.0738\}\end{aligned}$$

indicating the MOE becomes unstable by $M = 300$. Assuming that the values of the MOE are constant around $M = 30$ and taking the real part maximal eigenvalue of J as a function of M shows that a bifurcation takes place at $M \approx 31$ (Figure 3). It is also of interest to examine the effects of F and B on the stability of the MOE. Since the MOE is stable for $M = 30$, this is an acceptable value of M to investigate the effects of F and B. Figure 4 shows a bifurcation at approximately $F = 0.21$ when $M = 30$, identifying F as a bifurcation parameter. However, Figure 5 shows that the real part of the maximal eigenvalue of J is negative for any $B \in [1, 100]$ at $M = 30$, indicating that B is not a bifurcation parameter for this amount of morphine.

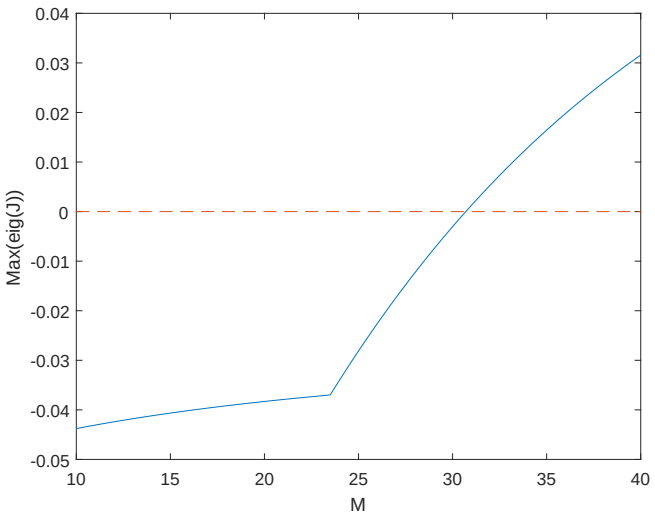

Figure 3. Effect of M on the stability of the MOE. The MOE becomes unstable at approximately $M = 31$.

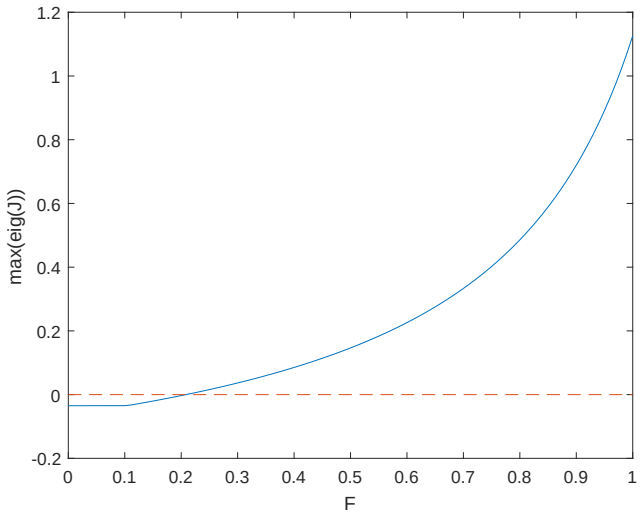

Figure 4. Effect of F on the stability of the MOE, $M = 30$. The MOE becomes unstable at approximately $F = 0.21$.

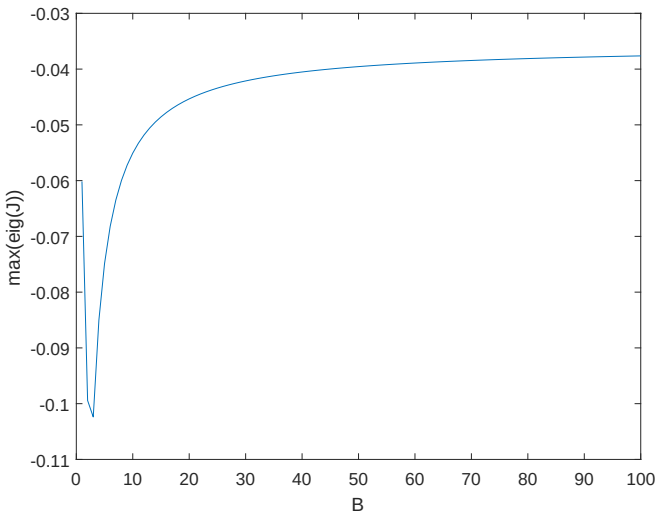

Figure 5. Effect of B on the stability of the MOE, $M = 30$. The MOE remains stable for this range of B.

Wild-type Only Equilbirum

A wild-type only equilibrium is a nonnegative solution of the form $(T_l^*, T_h^*, V_w^*, 0, I_w^*, 0, C^*)$ to the system of equations

$$\begin{aligned}
0 &= \lambda + qT_h - rT_l - \beta_l V_w T_l - \delta_T T_l \\
0 &= rT_l - qT_h - \beta_h V_w T_h - \delta_T T_h \\
0 &= pI_w - \delta_V V_w \\
0 &= (1-\hat{\epsilon})(\beta_l V_w T_l + \beta_h V_w T_h) - bI_w C - \delta_I I_w \\
0 &= \hat{\epsilon}(\beta_l V_w T_l + \beta_h V_w T_h) \\
0 &= \omega + \hat{\alpha} I_w C - \delta_C C.
\end{aligned}$$

Solving the second equation for T_h^* gives:

$$T_h^* \quad = \quad \frac{r}{q+\beta_h V_w^* + \delta_T} T_l^*$$

and the fifth equation is equivalent to

$$0 \quad = \quad \beta_l V_w T_l + \beta_h V_w T_h.$$

If $V_w^* = 0$ this system is exactly the IFE, so cancelling V_w^* and substituting T_h^* gives:

$$0 \quad = \quad T_l^* (\beta_l + \beta_h (\frac{r}{q+\beta_h V_w^* + \delta_T}))$$

so either $T_l^* = 0$ or $\beta_l + \beta_h (\frac{r}{q+\beta_h V_w^* + \delta_T}) = 0$. Substituting $T_l^* = 0$ into the first equation results in the negative solution $T_h^* = -\frac{\lambda}{q}$. Letting $\beta_l + \beta_h (\frac{r}{q+\beta_h V_w^* + \delta_T}) = 0$ is equivalent to

$$V_w^* \quad = \quad -\frac{1}{\beta_h} (\frac{\beta_h r}{\beta_l} + q + \delta_T)$$

which is also a negative solution, so there is no nonnegative wild-type only equilibrium.

CHAPTER 5

SIMULATIONS

This chapter will provide simulations of the system for various levels of morphine. The long-term viral load will be calculated for varying concentrations of morphine.

Short and Long Term Viral Dynamics

Using the initial values and parameters given in Chapter 3 along with $F = 0.2$, $B = 10$, $\psi = 0.05$ and $\mu = \eta = \gamma = \xi = 1$ the model is solved using the ode15s function in MATLAB over a period of 200 days and the total viral load $V_w + V_m$ is plotted on a log10 scale.

Whether or not morphine is present, the viral load rapidly increases to approximately 7.5 log10 before decreasing to a steady state of approximately 5.9 log10 for $M = 0$ and 6 log10 for $M = 300$ with a difference in viral load of approximately 2.18840×10^5 between the two cases (Figure 6). Decreasing B from 10 to 1 (Figure 7) increase the difference in the steady state viral load to 7.27520×10^5, which is closer to results obtained experimentaly [2].

As discussed in Chapter 4, a population switch occurs at $M \approx 31$ for the base parameter values. Therefore, it is of interest to observe the populations of the individual species in the cases where the wild-type dominates and in the case where the mutant dominates. Figure 8 separately shows the populations of the wild-type

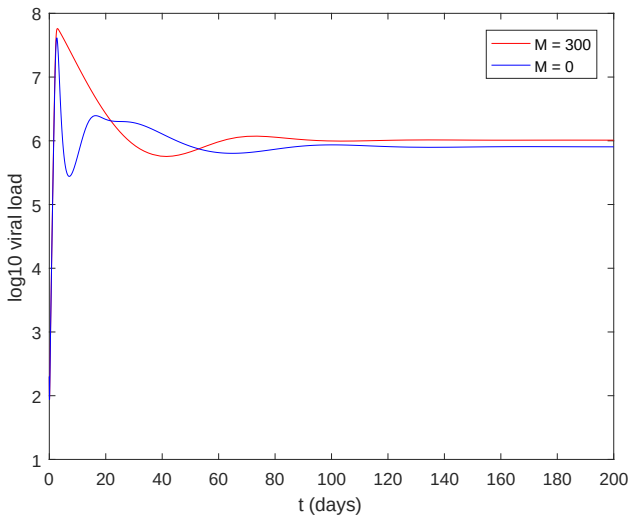

Figure 6. Total viral load with base parameter values. The model reflects the higher viral load caused by morphine.

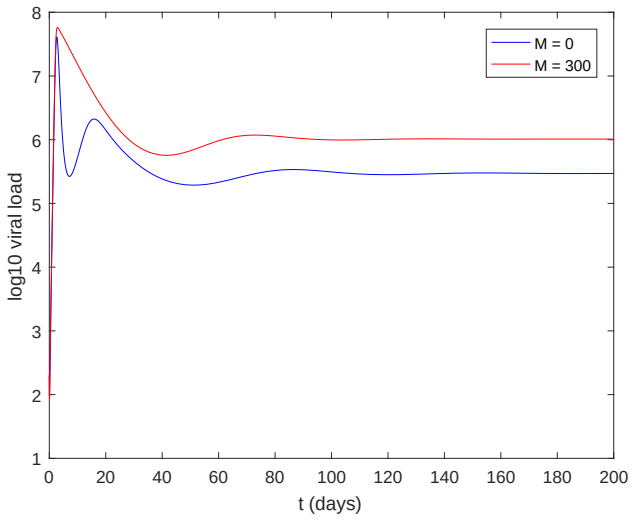

Figure 7. Total viral load with decreased escape ratio. Decreasing the escape ratio gives a differnce in viral load closer to experimental results.

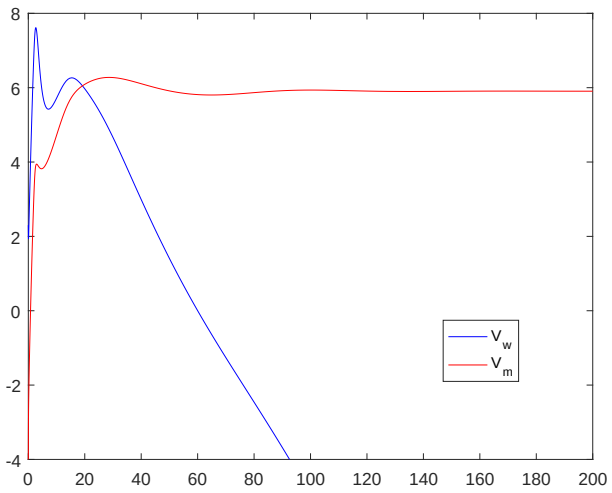

Figure 8. Individual virus populations, $M = 0$. When no morphine is present the mutant is the dominant species.

and mutant when $M = 0$. In this case, the logarithm of the wild-type virus becomes negative indicating that the wild-type population is approaching zero and the total viral load is essentially only the mutant population.

Figure 9 shows the individual populations for $M = 300$, a high enough morphine concentration for the wild-type to dominate. In this case the wild-type makes up the bulk of the viral load, however, due to mutation a small amount of mutant virus continues to be produced. These simulations are in agreement with the population switch discussed in Chapter 4.

Figure 10 shows the effect on the viral load at 200 days as a function of the

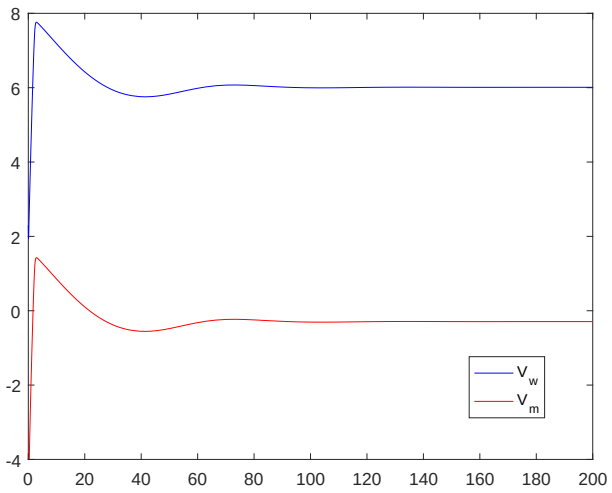

Figure 9. Individual virus populations, $M = 300$. For this amount of morphine the wild-type is the dominant species.

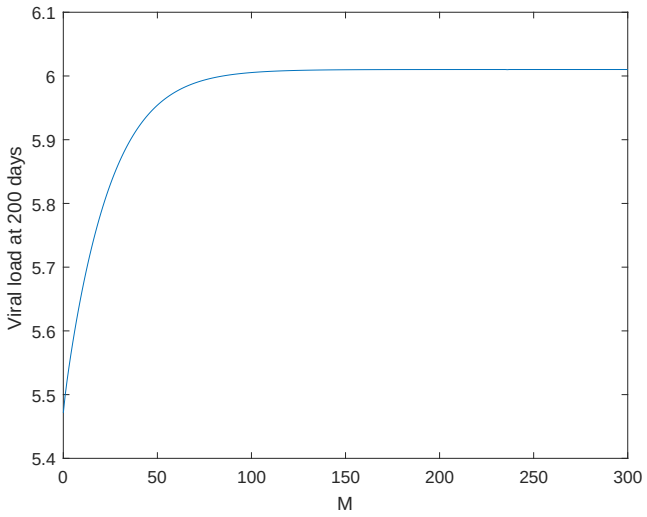

Figure 10. Viral load at 200 days as a function of M.

morphine concentration. There is a roughly 0.5 log10 difference in viral load between the $M = 0$ and $M = 300$ cases and the viral load is most sensetive to changes in M when $0 < M < 50$.

CHAPTER 6

DISCUSSION AND FUTURE WORK

Discussion

This thesis presents a mathematical model to describe the within-host viral dynamics of an HIV infection which considers escape mutants, the use of morphine, and different populations of target cells based on susceptibility to infection. The model is primarily based on earlier models from [21, 19] and simulates the increase in viral load that results from the use of morphine by introducing terms that lower the mutation rate of the virus and host's cellular immune response. Values of parameters in the model where taken both from earlier studies that provided estimates and from experimental data.

The basic reproduction number of each viral spiecies is calculated by way of the next-generation matrix method. The basic reproduction number was taken as a function of the concentration of morphine present and it was observed that a population switch occurs for a sufficiently high morphine concentration. At higher concentrations of morphine the wild-type virus dominates the mutant, but the reduced cellular immune response still results in a higher set point viral load. The infection free equilibrium is unstable regardless of whether or not morphine is present. The mutant only equilibrium is also stable for a sufficiently low morphine concentration and fitness cost of the virus, but becomes unstable as these parameters increase.

Short- and long-term viral dynamics are simulated by solving the model nu-

merically. If there is sufficient morphine for the wild-type virus to dominate a small amount of the mutant will persist due to mutation. If the mutant is the dominant species then it will effectively make up the entirety of the viral load. Varying the morphine concentration causes changes in the set point viral load for low concentrations, but the viral load stabilizes once the morphine concentration exceeds approximately $100ml/kg$.

One limitation of the model is the assumption that the morphine concentration M is constant with respect to time. This assumption is made for simplicity in calculations and for providing an easy way to determine the morphine concentration neccessary for the population switch to occur. Future work will focus on developing a method to incorporate a time-dependent morphine concentration and determining how this would affect the dynamics. It will also be of interest to investigate the sensitivity of the parameters introduced to model morphine effects, namely μ, η, γ and ξ, establish for them, and determining their effect on the stability of the equilbria of the model. Additionally, since it is possible for both the infection free and mutant only equilibria to be unstable it will be important to investigate any scenarios in which the wild-type and mutant coexist.

REFERENCES

1. *Morbidity and motality weekly report.* vol. 59 (2010) pp. 1550-1555.
2. R. Kumar, C. Torres, Y. Yamamura, I. Rodriguez, M. Martinez, S. Staprans, R. M. Donahoe, E. Kraiselburd, E. B. Stephens, and A. Kumar, *Modulation by morphine of viral set point in rhesus macaques infected with simian immunodeficiency virus and simian-human immunodeficiency virus*, J. Virol. vol. 78 (2004) pp. 11425-11428.
3. K. F. Hauser, Y. K. Hahn, V. V. Adjan, S. Zou, S. K. Buch, A. Nath, A. J. Bruce-Kelle, and P. E. Knapp, *HIV-1 tat and morphine have interactive effects on oligodendrocyte survival and morphology*, Glia vol. 57 (2009) pp. 194-206. doi:10.1002/glia.20746.
4. T. C. Greenough, D. B. Brettler, M. Somasundaran, D. L. Panicali and J. L. Sullivan, *Human immunodeficiency virus type 1- specific cytotoxic T lymphocytes (CTL), virus load, and CD4 T cell loss: evidence supporting a protective role for CTL in vivo*, J. Infect. Dis. vol. 176 (1997) pp. 118-125.
5. C. L. Boutwell, M. M. Rolland, J. T. Herbeck, J. I. Mullins, and T. M. Allen, *Viral evolutions and escape during acute HIV-1 infection*, J. Infect. Dis. vol. 202 (2010) pp. S309-S314.
6. A. S. Perelson and R. M. Ribeiro, *Modeling the within-host dynamics of HIV infection*, BMC Biol. (2013) http://www.biomedcentral.com/1741-7007/11/96
7. M. C. Chubb and K. H. Jacobsen, *Mathematical modeling and the epidemiological*

research process, Eur. J. Epidemiol. vol. 25 (2010) pp. 13-19.

8. S. G. Kitchen, J. K. Whitmire, N. R. Jones, Z. Galic, C. M. R. Kitchen, R. Ahmed, J. A. Zack, and F. V. Chisari, *The CD4 molecule on CD8+ T lymphocytes directly enhances the immune response to viral and cellular anitgens*, Proc. Natl. Acad. Sci. U.S.A. vol. 102 (2005) pp. 3794-3799.
9. N. Kileen, C. B. Davis, K. Chu, M. E. C. Crooks, S. Sawada, J. D. Scarborough, K. A. Boyd, S. G. Stuart, H. Xu, and D. R. Littman, *CD4 function in thymocyte differentiation and T cell activation*, Philos. Trans. R. Soc. Lond., B, Biol. Sci. vol. 342 (1993) pp. 25-34.
10. D. C. Chan and P. S. Kim, *HIV entry and its inhibition*, Cell. vol. 93 (1998) pp. 681-684.
11. A. S. Fauci, *Pathogensis of HIV disease: Opportunities for new prevention interventions*, Clin. Infect. Dis. vol. 45 (2007) pp. S206-S212.
12. A. J. McMichael and S. L. Rowland-Jones, *Cellular immune responses to HIV*, Nature vol. 410 (2001) pp. 980-987.
13. L. Deng, M. Pertea, A. Rongvauz, L. Want, C. M. Durand, G. Ghiaur, J. Lai, H. L. McHugh, H. Hao, J. B. Margolick, C. Gurer, A. J. Murphy, D. M. Valenzuela, G. D. Yancopoulus, S. G. Deeks, T. Stowig, P. Kumar, J. D. Siliciano, S. L. Salzberg, R. A. Flavell, L. Shan, and R. F. Siliciano, *Broad CTL response is required to clear latent HIV-1 due to dominance of escape mutations*, Nature vol. 517 (2015) pp. 381-385.
14. R. M. Ribeiro, L. L. Chavez, D. Li, S. G. Self, and A. S. Perelson, *Estimation of the initial viral growth rate and basic reproductive number during acute HIV-1*

infection, J. Virol. vol. 84 (2010) pp. 6096-6102.

15. Y. Li, X. Wang, S. Tian, C. Guo, S. D. Douglas, and W. Ho, *Methadone enhances human immunodeficiency virus infection of human immune cells*, J. Infect. Dis. vol. 185 (2002) pp. 118-122.
16. R. Noel, Z. Marrero-Otero, R. Kumar, G. S. Chompre-Gonzalez, A. S. Verma, and A, Kumar, *Correlation between SIV tat evolution and AIDS progression in cerebrospinal fluid of morphine-dependent and control macaques infected with SIV and SHIV*, Virology vol. 349 (2006) pp. 440-452.
17. R. Noel and A. Kumar, *SIV vpr evolution is inversely related to disease progression in a morphine-dependent rhesus macaque model of AIDS*, Virology vol. 359 (2007) pp. 397-404.
18. V. Rivera-Amill, P. S. Silverstein, R. Noel, S. Kumar, and A. Kumar, *Morphine and rapid disease progression in nonhuman primate model of AIDS: Inverse correlation between disease progression and virus evolution*, J. Neuroimmune Pharmacol vol. 5 (2014) pp. 122-132. http://doi.org/10.1007/s11481-009-9184-0
19. B. P. Konrad, N. K. Vaiyda, and R. J. Smith?, *Modeling mutation to a cytotoxic T-lymphocyte HIV vaccine*, Math. Popul. Stud. vol. 18 (2011) pp. 122-149.
20. E. S. Schwartz, K. R. H. Biggs, C. Bailes, K. A. Ferolito, and N. K. Vaidya, *HIV dynamics with immune responses: Perspectives from mathematical modeling*, Curr. Clin. Microbiol. Rep. vol. 3 (2016) pp. 216-224.
21. N. K. Vaidya, R. M. Ribeiro, A. S. Perelson, and A. Kumar, *Modeling the effects of morphine on simian immunodeficiency virus dynamics*, PloS Comput. Biol. (2016) https://doi.org/10.1371/journal.pcbi.1005127

22. C. Castillo-Chavez, Z. Feng, and W. Huang, *On the computation of R_0 and its role on global stability*, Mathematical Approaches for Emerging and Reemergin Infections Diseases: An Introduction, Springer-Verlag, New York, 2002, pp. 229-250.

23. K. T. Olkkola, E. Maunuksela, R. Korpela, and P. H. Rosenberg, *Kinetics and dynamics of postperative intravenous morphine in children*, Clin. Pharmacol. Ther. vol. 44 (1988) pp. 128-136.

24. L. Perko, *Differential equations and dynamical systems*, 2nd ed., Springer-Verlag, New York, 1991.

25. D. W. Jordan and P. Smith, *Nonlinear ordinary differential equations: An introduction to dynamical systems*, 3rd ed. Oxford University Press, New York, 1999.

26. V. V. Ganusov and R. J. De Boer, *Estimating costs and benefits of CTL escape mutations in SIV/HIV infection*, PloS Comput. Biol.(2006) https://doi.org/10.1371/journal.pcbi.0020024

27. R. J. Smith and L. M. Wahl, *Drug resistance in an immunological model of HIV-1 infection with impulsive drug effects*, Bull. Math. Biol. vol. 67 (2005) pp. 783-813.

28. D. H. Barouch, J. Kunstman, J. Glowczwskie, K. J. Kunstman, M. A. Egan, F. W. Peyerl, S. Santra, M. J. Kuroda, J. E. Schmitz, K. Beaudry, G. R. Krivulka, M. A. Lifton, D. A. Gorgon, S. M. Wolinsky, and N. L. Letvin, *Viral escape from dominant simian immunodeficiency virus epitope-specific cytotoxic T lymphocytes in DNA-caccinated rhesus monkeys*, J. Virol. vol. 77 (2003) pp. 7367-7375.

29. B. Ramratnam, S. Bonhoeffer, J. Binley, A. Hurley, L. Zhang, J. E. Mittler, M. Markowitz, J. P. Moore, A. S. Perelson, and D. D. Ho, *Rapid production and clearance of HIV-1 and hepatitis C virus assessed by large volume plasma apheresis*, Lancet. vol. 354 (1999) pp. 1782.

30. M. A. Stafford, L. Corey, Y. Cao, E. S. Daar, D. D. Ho, and A. S. Perelson, *Modeling plasma virus concentration during primary HIV infection*, J. Theor. Biol. vol. 203 (2000) pp. 285-301.

31. L. M. Mansky and H. M. Temin, *Lower in vivo mutation rate of human immunodeficiency virus type 1 than that predicted from the fidelity of purified reverse transcriptase*, J. Virol. vol. 69 (1995) pp. 5087-5094.

32. S. Marino, I. B. Hogue, C. J. Ray, and D. E. Kirschner, *A methodology for performing global uncertainty and sensitivity analysis in systems biology*, J. Theor. Biol. vol. 254 (2008) pp. 178-196.

33. R. J. De Boer and A. S. Perelson, *Target cell limited and immune control models of HIV jnfection: A comparison*, J. Theor. Biol. vol. 190 (1998) pp. 201-214.

34. O. Diekmann, J. A. P. Heesterbeek, and M. G. Roberts, *The construction of next-generation matrices for compartmental epidemic models*, J. R. Soc. Interface (2009) http://rsif.royalsocietypublishing.org/content/7/47/873

35. S. D. Perera, S. S. N. Perera, and S. Jayasinghe, *Modeling and sensitivity of dengue viral dynamics*, Int. J. Curr. Res. vol. 8 (2006) pp. 34899-34906.

36. H. S. Rodrigues, M. T. T. Monteiro, and D. F. M. Torres, *Sensitivity analysis in a dengue epidemiological model*, Conference Papers in Mathematics vol. 2013 (2013).

VITA

Peter Uhl was born on December 12, 1991 in Kansas City, Missouri. He graduated from Shawnee Mission East High School in 2010 and received a bachelor's degree in mathematics and statistics from the University of Missouri-Kansas City in 2015.